Separation of cells and microparticles in insulator-based electrokinetic systems

3

4 Alaleh Vaghef-Koodehi, † Olivia D. Ernst† and Blanca H. Lapizco-Encinas†,*

5

[†] Microscale Bioseparations Laboratory and Biomedical Engineering Department, Rochester Institute of
 [†] Technology, 160 Lomb Memorial Drive, Rochester, New York, 14623, United States;

8 9

10

11

Keywords:

- 12 Cells
- 13 Electrokinetics
- 14 Electrophoresis
- 15 Microfluidics
- 16 Separations

ABSTRACT: Presented here is the first continuous separation of microparticles and cells of similar characteristics employing linear and nonlinear electrokinetic phenomena in an insulator-based electrokinetic (iEK) system. By utilizing devices with insulating features, which distort the electric field distribution, it is possible to combine linear and nonlinear EK phenomena; resulting in highly effective separation schemes, that leverages the new advancements in nonlinear electrophoresis. This work combines mathematical modeling and experimentation to separate four distinct binary mixtures of particles and cells. A computational model with COMSOL Multiphysics was used to predict the retention time $(t_{R,p})$ of the particles and cells in iEK devices. Then, the experimental separations were carried out using the conditions identified with the model, where the experimental retention time $(t_{R,e})$ of the particles and cells was measured. A total of four distinct separations of binary mixtures were performed by increasing the level of difficulty. For the first separation, two types of polystyrene microparticles, selected to mimic E. coli and S. cerevisiae cells, were separated. By leveraging the knowledge gathered from the first separation, a mixture of cells of distinct domains and significant size differences, E. coli and S. cerevisiae, were successfully separated. The third separation also featured cells of different domains, but closer in size: B. cereus vs. S. cerevisiae. The last separation included cells in the same domain and genus, B. cereus vs. B. subtilis. Separation results were evaluated in terms of the number of plates (N) and separation resolution (Rs), where Rs values for all separations were above 1.5, illustrating complete separations. Experimental results were in agreement with modeling results in terms of retention times, with deviation in the 6%-27% range; while the variation between repetitions was between 2%-18%, demonstrating good reproducibility. This report is the first prediction of the retention time of cells in iEK systems.

32 33

34

35

36

37

38

39

40

41

42

43

44

45

46

47

48

49

50

51

52

53

54

55

56

57

58

59

60

61

17

18

19 20

21

22

23

24

25

2627

28

29 30

31

Traditional techniques for analyzing nano-sized bioparticles (e.g., capillary electrophoresis and chromatography) are well-established and reliable. However, there is a lack of similarly reliable methods for separating and identifying micron-sized bioparticles, such as microorganisms. Only a handful groups, such as the Horká²⁻⁴ and Buszewski⁵⁻⁸ groups, have recently investigated the separation of microorganisms with traditional electrophoretic techniques, an area that was pioneered by Armstrong in 1999.9 The Horká and Buszewiski have made important advancements, such as the separation between antibiotic resistant and antibiotic susceptible bacteria, isolation and propagation of bacteriophages, effect of electrolyte pH, evaluation of bacterial aggregations, 8 etc. Although electrophoresis-based separations offer an attractive alternative for the rapid detection and separation of microbes, their applications is not widespread. There is a growing interest in the development of rapid techniques for the analysis of microorganisms, as conventional culture-based and filtration methods are laborintensive, time-consuming, and have low efficiency. Microfluidic technologies have proven to be effective platforms for the manipulation and assessment of a wide range of nano- and microparticles of interest. 1,10 Microscale electrokinetics (EK) has become one of the main pillars of microfluidics due to its robustness and flexibility, 10,11 that allows implementing hybrid systems with higher integration. 12,13 Linear and nonlinear EK phenomena have been employed for designing effective separation processes. In iEK systems, the presence of the insulating structures within a microchannel distorts the electric field distribution when a potential is applied to the channel, creating zones of higher and lower field intensity, which yields iEK systems with the unique ability to combine linear and nonlinear phenomena within a single system. ^{14,15,16} If the insulating posts were not present, there would be no regions of higher field intensity in the microchannel, and thus, nonlinear effects would not arise at the low voltages employed for these separations. Recently, Khair¹⁷ stated that during the last century the fundamentals of linear electrophoresis were established. In contrast, during the 21st century, in particular the last decade, major advances have been reported on nonlinear electrophoresis of colloidal particles. There are major opportunities to develop powerful separation schemes for colloidal particles such as beads and cells, by exploiting the potential of nonlinear electrophoresis, opening the possibilities to carry out separations that are not possible employing traditional linear electrophoretic approaches.¹⁷ Insulator-based EK (iEK) devices have the capability to separate complex samples, including cells of similar characteristics, ^{18–20} by employing a strategic combinations of linear and nonlinear EK effects. Numerous successful applications of iEK devices have been reported, including enrichment of DNA, 21 sorting of cell organelles, 16 separations of exosomes, 22 differentiation between bacterial and

yeast cells, ^{23,24} analysis of neural stem cells²⁵ and the separation of tumor cells. ²⁶

62

63

64

65

66

67

68

69

70

71

72

73

74

75

76

77

78

79

80

81

82

83

84

85

86

87

88

89

90

91

92

93

94

95

96

97

98

99

100

101

102

103104

The Hayes research group has published numerous reports on the technique of gradient insulator-based dielectrophoresis (g-iDEP), which employs devices with sawtooth insulating walls. They have worked extensively with bacterial cells and viruses. ^{27,28} The unique insulating tooth structures create an increasing electric field gradient across the length of the g-iDEP microchannels, which has allowed them to isolate and trap microorganisms at specific channel locations. They have reported the differentiation between Escherichia coli (E. coli) cells with the same serotype, ²³ examined the trapping behavior of three serovars of *Listeria monocytogenes* (*L. monocytogenes*), ²⁹ and simultaneously captured and concentrated resistant Staphylococcus epidermidis (S. epidermidis) vs. susceptible S. epidermidis.³⁰ The Agah research group reported iEK separations of cells and microparticles employing a DCbiased high-frequency AC electric field in a device with 3D constrictions to trap E. coli in a mixture of polystyrene particles³¹ and separate dead and living Staphylococcus aureus (S. aureus) cells.³² The Buie group also utilized a 3D approach to trap E. coli and Bacillus cereus (B. cereus) cell, and found that systems with 3D constrictions require lower voltages, thus reducing Joule heating effects. The same method was used to discriminate between the strains of pathogenic Streptococcus mitis (S. mitis) and Pseudomonas aeruginosa (P. aeruginosa). 33 The Lapizco research group has published several studies on EK separations of microparticles and cells in an array of iEK systems.^{24,34–37}A recent study illustrated that carefully selected operating conditions and accurate mathematical modeling allowed for the successful separation of almost identical microparticles with a slight difference in electrical charge of only 3.6 mV.³⁸ Several studies by this group have targeted the separation and trapping of mixtures of cells. In 2010, they reported the simultaneous separation and centration of a mixture of yeast and E. coli cell in an iEK system in less than 2 minutes.³⁹ In 2016, this group proposed the combination of asymmetric insulating posts and asymmetric DC-biased low-frequency AC fields, which allowed them to separate a mixture of particles and cells by selectively eluting the more fragile and larger yeast cells.²⁴ In three recent studies, ^{37,40,41} this group analyzed the effect of nonlinear electrophoresis and the concept of the Electrokinetic Equilibrium Condition (EFFC) on the migration and trapping behavior of bacterial and yeast cells. Other iEK approaches have been developed for the sorting and enrichment of cells and microparticles. The Li group developed systems with single insulating hurdle, 42 which was extended by the Ros group with their work with single constriction sorter devices. 20 The Xuan group developed the technique of curvature-induced dielectrophoresis (c-DEP)⁴³⁻⁴⁵ and reservoir-based DEP (rDEP). The Thöming group reported mesh-based DEP filter for shape-based separation of microparticles⁴⁶ and a switchable DEP filter for separating submicron particles.⁴⁷ Hybrid methods have also been proposed, for instance the combination of iEK and determinist lateral displacement (DLD) developed by the Morgan group. 48,49

The present work is the first report of the separation of binary mixtures of polystyrene microparticles and bacterial and yeast cells in a continuous mode using an iEK device with asymmetrical insulating posts that allows combining linear and nonlinear EK effects. This study aims to push the discriminatory capabilities of iEK systems and demonstrate effective separations of cells with a novel iEK-based approach that leverages the new advancements in nonlinear electrophoresis. 17,18,50,51 A combination of mathematical modeling with COMSOL *Multiphysics* and experimentation was employed to design four distinct separations. First, COMSOL predictions of particle retention time ($t_{R,p}$) in the iEK channel allowed obtaining the appropriate electrical potentials used to separate each binary mixture by considering the particles/cells characteristics and identifying if the separation should occur under linear or nonlinear EK regimes. Then, experiments were performed to separate the mixtures of particle or cells and determine the experimental retention time ($t_{R,e}$). The four distinct separations were performed with an increasing level of difficulty. The first separation featured two types of polystyrene microparticles (2 µm and 5.1 µm in diameter), which were strategically selected to mimic *E. coli* and *Saccharomyces cerevisiae* (*S. cerevisiae*) cells. With the knowledge acquired from the microparticle separation, the second separation

demonstrated the discrimination between $E.\ coli$ and $S.\ cerevisiae$, which are cells of distinct domains, prokaryotic and eukaryotic, respectively, that vary significantly in size. The third separation between $B.\ cereus$ vs. $S.\ cerevisiae$ proved that cells of distinct domains, closer in size, can also be successfully separated in matter of minutes. The fourth separation illustrated the distinction between cells of the same domain and same genus, by separating $B.\ cereus$ vs. $Bacillus\ subtilis\ (B.\ subtilis)$ cells. There was good agreement between COMSOL predicted retention times $(t_{R,p})$ and experimentally determined retention times $(t_{R,p})$, with deviations in the 6-27% range. Experimental results had high reproducibility, with deviations between repetitions in the 2-18% range. All separations had a resolution Rs > 1.5, revealing the potential of iEK systems for the analysis of micron-sized particles, including microorganisms. The separation method proposed here leverages the developments on linear electrophoresis from the last century and the recent advances in nonlinear electrophoresis, creating an effective separation scheme with high resolution capable of distinguishing between high similar particles and cells. This novel makes enables separations of highly similar particles and cells that are not possible with traditional electrophoretic approaches. This report is the first prediction of the retention time of cells in continuous iEK separations with a mathematical model that did not require the use of empirical correction factors, achieving good agreement between modeling and experimental results.

THEORY

Electrokinetic phenomena are classified as linear and nonlinear, according to their dependence on the electric field. The ability of combining linear and nonlinear EK phenomena within the same device is an advantageous characteristic of iEK systems. When an electric potential is applied, the presence of the insulating structures or posts in the channel distort the electric field distribution, creating zones of higher field intensity, where nonlinear EK effects can arise. Under weak electric fields, the two phenomena acting on the migration of particles in iEK systems are linear electrophoresis (EP⁽¹⁾) and electroosmosis (EO), for which the velocity expressions are: 14,15,18

$$\mathbf{v}_{EO} = \mu_{EO} \mathbf{E} = -\frac{\varepsilon_m \zeta_W}{\eta} \mathbf{E} \tag{1}$$

128
$$\mathbf{v}_{EP,L} = \mu_{EP,L} \mathbf{E} = \frac{\varepsilon_m \zeta_P}{n} \mathbf{E}$$
 (2)

where \mathbf{v} is velocity, μ is mobility, ε_m and η are the electrical permittivity and viscosity of the suspending medium, ζ is the zeta potential for either the channel wall or the microparticle, and \mathbf{E} is the electric field. The nonlinear EK phenomena considered here are dielectrophoresis (DEP) and nonlinear EP, also called EP of the second kind, denoted as $\mathrm{EP}^{(3)}$ to illustrate a cubic dependence of the nonlinear EP velocity on the electric field under the selected operating conditions (see **Table S1**⁵¹). The velocity expressions for these two nonlinear phenomena are: 14,15,18

134
$$\mathbf{v}_{DEP} = \mu_{DEP} \nabla E^2 = \frac{r_p^2 \varepsilon_m}{3\eta} \operatorname{Re}[f_{CM}] \nabla E^2$$
 (3)

135
$$\mathbf{v}_{EP,NL}^{(3)} = \mu_{EP,NL}^{(3)} \mathbf{E}^3$$
 (4)

where $Re(f_{CM})$ is the real part of the Clausius-Mossotti factor, which describes particle polarization, and r_p is the diameter of the microparticle. The expression of the overall particle velocity (\mathbf{v}_P) , considering all four EK phenomena, can be written as follows:

139
$$\mathbf{v}_P = \mathbf{v}_{EO} + \mathbf{v}_{EP,L} + \mathbf{v}_{DEP} + \mathbf{v}_{EP,NL}^{(3)} = \mu_{EO} \mathbf{E} + \mu_{EP,L} \mathbf{E} + \mu_{DEP} \nabla E^2 + \mu_{EP,NL}^{(3)} \mathbf{E}^3$$
 (5)

Recent studies^{18,37} have proven that the influence of DEP on the overall particle velocity are not significant in

systems stimulated with DC and low-frequency AC fields, thus, the expression in Equation (5) could be further simplified by removing the \mathbf{v}_{DEP} term.

The quality of each one of the binary separations was evaluated by estimating the separation resolution (Rs) and the number of plates (N) of the electropherograms of the separations. The following expressions were employed, where t_R and W are the retention time and the width of the peak at the base, respectively.

$$Rs = \frac{2(t_{R2} - t_{R1})}{W_1 + W_2} \tag{6}$$

$$N = \frac{16 \ t_{R,e}^2}{W^2} \tag{7}$$

EXPERIMENTAL SECTION

Suspending Medium. A 0.2 mM buffer solution of K_2HPO_4 , with the addition of 0.05% (v/v) Tween 20 to prevent particle adhesion, was used as the suspending medium, which resulted in a conductivity of 40.7 μ S/cm and pH of 7.3. Using current monitoring experiments,⁵² a wall zeta potential (ζ_W) of -60.1 mV and $\mu_{EO} = 4.7 \times 10^{-8} m^2 V^{-1} s^{-1}$ were characterized for this suspending medium for all polydimethylsiloxane (PDMS) surfaces, including the microchannel walls and the surface of the insulating posts

Microparticle and Cell Samples. Table 1 lists the properties of the polystyrene microparticles used in this work (Magsphere Pasadena, CA, USA). Microsphere sample suspensions were prepared by diluting concentrated particles into the suspending medium solution. Additionally, four types of cells were studied in this work: *E. coli* (ATTC 11775), *B. cereus* (ATCC 14579), *B. subtilis* (ATCC 6051), and *S. cerevisiae* (ATCC 9763). The properties of the cells are listed in **Table 1**. All cells were cultured and stained following standard procedures employing fluorescent SYTO dyes (Thermofisher, Carlsbad, CA).³⁷. The values of ζ_P , $\mu_{EP,L}$ and $\mu_{EP}^{(3)}$ listed in **Table 1** were obtained with particle tracking velocimetry (PTV) experiments.^{18,40} All cells and particles in this study had a negative surface charge. The operating conditions and results obtained in each one of the separations are listed in **Table 2** and **Table 3**, respectively. It is worth mentioning that cells retained their variability after the treatment with the electric potential, as demonstrated in a previous study by our group.⁵³

Table 1. Characteristics for microparticles and cells used in this study.

ID	Size (µm)	$\frac{\zeta_P}{(\mathbf{mV})}$	$\mu_{EP}^{(1)} \times 10^{-8}$ (m ² V ⁻¹ s ⁻¹)	E for $\mu_{EP}^{(3)}$ estimation (V/cm)	$\mu_{EP}^{(3)} \times 10^{-18}$ (m ⁴ V ⁻³ s ⁻¹)
Particle 1-red	2.0 diameter	-11.5 ± 0.6	$\textbf{-0.9} \pm 0.1$	400 ± 100.0	-10.1 ± 0.4
Particle 2-green	5.1 diameter	-31.4 ± 1.1	-2.4 ± 0.1	200 ± 50.0	-6.4 ± 3.2
E. coli (ATTC 11775)	$2.38 \pm 0.32 \text{ long}$ $0.96 \pm 0.21 \text{ wide}$	-25.4 ± 1.5	-2.0 ± 0.1	500 ± 100.0	-7.4 ± 2.3
S. cerevisiae (ATCC 9763)	6.23 ± 0.77 diameter	-29.1 ± 3.7	-2.2 ± 0.2	150 ± 50.0	-64.1 ± 9.4
B. cereus (ATCC 14579)	$4.9 \ 4 \pm 0.47 \ long$ $1.32 \pm 0.13 \ wide$	-46.1 ± 3.1	-3.5 ± 0.2	250 ± 50.0	-4.2 ± 3.4
B. subtilis (ATCC 6051)	4.86 ± 0.41 long 1.94 ± 0.19 wide	-30.0 ± 5.8	-2.34 ± 0.4	200 ± 50.0	-41.6 ± 31.0

Microdevices. Microdevices with T-shaped microchannels, a standard configuration for EK injection, were made with PDMS (Dow Corning, MI, USA) following standard soft lithography techniques.²⁴ All devices featured a 51.5 mm long main channel and a 22 mm long secondary channel. All channels were 1.1 mm wide and 40 μm deep. Channel and post dimensions are detailed in **Figure 1A**. Asymmetric posts were utilized, as previous studies have shown that this configuration has enhanced discriminatory capacity.^{24,34}

Equipment and Software. LabSmith Sequencer software was used to control a high voltage power supply (Model HVS6000D, LabSmith, Livermore, CA) used to apply DC voltage to the microchannels through platinum electrodes. Experimental sessions were recorded on a Zeiss Axiovert 40 CFL (Carl Zeiss Microscopy, Thornwood, NY) and a Leica DMi8 (Wetzlar, Germany) inverted microscopes.

Mathematical Modeling. Prior to the separation experiments, predictions of particle/cell retention time ($t_{R,p}$) were carried out employing a mathematical model built with COMSOL *Multiphysics*. The model employed the particle/cell properties listed in **Table 1**, which were obtained *a priori* with PTV measurements, ^{18,40} *i.e.*; characterization of the particles/cells is required to in order to model the performance of the separation in terms of retentions times. The application of this iEK method require COMSOL modeling to determine the voltages to be used to achieve a successful separation and to determine if the separation should take place under linear or nonlinear regimes. The COMSOL model allowed selecting the appropriate voltages to be used to effectively discriminate between the two distinct particles/cells in each binary mixture and achieve a Rs > 1.5. Details on the COMSOL model are included in the supplementary information (**Figure S1**, **Table S2**, and **Figure S2**). The detailed model results, in terms of $t_{R,p}$, are also included in the supplementary information (Tables S3-S6).

Experimental Procedure. Prior to experiments the microchannels (Figure 1A) were filled with the suspending medium. The effects of pressure-driven flow were minimized by employing large liquid reservoirs (~4 mL) at the inlets and outlets of the channel. Particle or cell sample suspensions (10 μL) were introduced into the inlet reservoir (Inlet A in Figure 1A), and then platinum wire electrodes were placed at each reservoir. Samples were introduced employing a standard 3-step EK injection process. The voltages applied and time duration of the EK injection steps are listed in Table 2. The last step in each separation was determined by the elution of the particle/cell peaks from the channel. The fluorescence signal of each eluting peak was captured at the end of the post array as shown in Figure 1A. All separations were repeated at least three times to ensure reproducibility (Table S7).

Table 2. Voltages employed for EK sample injection and iEK-based separations.

Separation ID	Description	Particle or cell concentration x 10 ⁸ (#/mL)	Step	Run time (s)	Applied voltage (V) in each reservoir			
					A	В	C	D
1	Separation of microparticles: red (2 μm) and green (5.1 μm)	Red: 2.2 Green: 0.6	Loading Gating Injection	22 2 200	600 1500 0	300 1500 1500	0 1200 0	500 0 0
2	Separation of cells of different domains: <i>E. coli</i> vs. <i>S. cerevisiae</i>	E. coli: 4.5 S. cerevisiae: 1.0	Loading Gating Injection	30 5 400	500 1000 0	300 1000 1000	0 1000 0	500 0 0
3	Separation of cells of different domains: <i>S. cerevisiae</i> vs. <i>B. cereus</i>	S. cerevisiae: 0.6 B. cereus: 1.7	Loading Gating Injection	10 5 400	500 1500 200	300 1500 500	0 1500 200	600 0 0
4	Separation of cells of the same genus: <i>B. subtilis</i> vs. <i>B. cereus</i>	B. subtilis: 3.0 B. cereus: 2.0	Loading Gating Injection	30 5 600	500 1500 200	300 1500 500	0 1500 200	500 0 0

199

200

201

202

203

204

205

206

207

208

209

210

211

212

213

214

215

216

217

218

219

220

221

222

Table 3. Separation results: separation resolution, predicted and experimental retention time values, deviation of COMSOL results from experimental results, and deviation between three repetitions for each separation.

Separation ID	Particle ID	Rs	COMSOL predicted $t_{R,p}$ (s)	Experimental $t_{R,e}(s)$	Deviation $t_{R,p}$ vs. $t_{R,e}$ (%)	Deviation in repetitions (%)
1	Particle 1-Red		63	50	-27	18
	Particle 2-Green	3.38	102	138	26	3
2	E. coli (green, ATTC 11775)	2.12	132	166	20	2
	S. cerevisiae (red, ATCC 9763)	2.13	169	230	27	2
3	S. cerevisiae (red, ATCC 9763)		179	152	-18	7
	B. cereus (green, ATCC 14579)	3.52	357	411	13	7
4	B. subtilis (ATCC 6051)		180	170	-6	6
	B. cereus (ATCC 14579)	4.79	357	460	22	13

RESULT AND DISCUSSION

Separation of Microparticles that Mimic Cells. The goal of this separation of two types of polystyrene microparticles was to gain knowledge to separate a mixture of E. coli and S. cerevisiae cells. In this separation, the 2 μm red particles are substitutes for E. coli, and the 5.1 μm green particles are substitutes for S. cerevisiae. Employing the particle properties listed in **Table 1**, the 2D COMSOL model was used to estimate $t_{R,p}$ values for each particle in a range of applied voltages (see Table S3) for the third (injection) step of the EK injection process. After analyzing the COMSOL predictions, the voltages listed in **Table 2** for Separation 1 were selected, as according to the model, these voltages should produce well-resolved peaks (Rs > 1.5). It is important to mention that the COMSOL model employed here considers the effects of nonlinear EP, a phenomenon that had been ignored in the modeling of many iEK systems stimulated with DC and low-frequency AC potentials. 14,38 The accuracy of this model has enabled the design of challenging separations, our group recently reported the separation of two types almost identical microparticles.³⁸ The results of Separation 1, the mixture of the 2 µm red and 5.1 µm green particles, are shown in Figure 1B-C. The image in Figure 1B shows the particles as they migrate across the asymmetric insulating post array forming "zones," with the 2 µm red particles moving ahead of the green 5.1 µm particles at $\Delta V = 1500 V$ between reservoirs B and D. Figure 1C presents the electropherogram of this separation, which was built from the fluorescence signal from the particles as they eluted the post array. As expected from observing the particle "zones," the red particles eluted first ($t_{R1,e} = 50 \text{ s}$), followed by the green particles ($t_{R1,e} = 50 \text{ s}$) 138 s). The results from three distinct repetitions are reported in **Table S7**, and the deviation between repetitions was less than 18% for the red particles and 3% for the green particles. These experimental $t_{R,e}$ values are in fair agreement with predicted $t_{R,p}$ values, which are $t_{R1,p} = 62$ s and $t_{R2,p} = 103$ s for red and green particles, respectively. Linear EK forces are the main mechanisms behind this separation. By looking at the microparticle properties in **Table 1**, the values of ζ_P explain these results. The red particles have a lower magnitude ζ_P and $\mu_{EP,L}$, which means that they experience a lower EP force towards the inlet, and thus, and have a higher overall velocity (\mathbf{v}_P) towards the outlet. This higher velocity allows them to migrate across the entire post array faster than the green

particles, as clearly illustrated in Figure 1B-1C. Since these two particles had a difference of ~20 mV in the magnitudes of their ζ_P values, this separation was designed to be carried out in the linear EK regime. Care was taken to avoid nonlinear EP effects, since the magnitudes of the $\mu_{EP,NL}^{(3)}$ mobilities would favor the opposite elution order, i.e., the green particle to be eluted first, as it has the lower magnitude $\mu_{EP,NL}^{(3)}$. To further analyze the relative effect of the each one of the four linear and nonlinear EK phenomena considered here, COMSOL simulations were utilized to predict the overall particle velocity and the individual velocities exerted by each EK phenomena on a particle/cell migrating across one constriction between two insulating posts. The velocity predictions are shown in Figure S3 for all four separations included in this study. In the case of Separation 1, Figure S3A-3B illustrates that the separation was dominated by the two linear EK phenomena: linear EO and EP, since as mentioned, linear EK favors the selected particle elution order. As observed in Figure 1C, the red and green peaks are well defined, although peak overlapping can be seen as the result of co-elution of the two types of particles. This co-elution can be caused by the highly concentrated sample employed, which results in particle interactions that further distort the electric field distribution. While these separation experiments require highly concentrated samples, these particles/cells act as insulators creating localized zones of high electric field strength, which in turn affects the local particle velocity, accelerating some particles and causing co-elution. This is observed in the electropherograms as particle leakage as seen in **Figure 1C**. This separation had a resolution of Rs = 3.38 (Equation 6), which confirms an effective separation. The separation efficiency was also evaluated in terms of number of plates per meter (N/m)Equation 7) for each peak, with the following $N_1/m = 1,749$ plates/m and $N_2/m = 24,785$ plates/m for red and green particles, respectively. These results in terms of N/meter are comparable to those obtained with traditional capillary electrophoresis CE systems, which have been reported in the range of 1,830 to 11,800 plates/meter in devices for protein characterization.⁵⁴ Good reproducibility was obtained with this separation, with deviation of between repetitions in terms of $t_{R,e}$ of 18% and 3% for Particle 1 and Particle 2, respectively (**Table S7**).

Regarding the agreement between the mathematical model and experiments, the results are encouraging, as both particles showed deviations below 30% between their $t_{R,p}$ vs. $t_{R,e}$, the deviations were -27% for red particles and 26% for green particles. There are several potential possibilities to explain these deviations, such as effects of "injection bias" in the EK injection process used to introduce the particles into the channel, which would favor the red particles as they have a greater overall migration forward. Another potential cause of deviation between modeling and the experimental results can be particle-particle interactions caused by the relatively high particle concentration. The mathematical model does not currently account for the effect of injections bias and particle-particle interactions. Considering this, and the fact that no empirical correction factors were employed, the COMSOL model is an effective tool for designing particle separations.

Separation of the Cells of Different Domains Mimicked in the Previous Separation: *E. coli* and *S. cerevisiae*. The second separation analyzed a binary mixture of *E. coli* (green) and *S. cerevisiae* (red) cells, which were mimicked by employing polystyrene particles in Separation 1. The COMSOL model was employed to predict the migration of cells within the separation channel for a range of applied voltages (**Table S4**). Based on the computational model, since the ζ_P of *E. coli* is -25.4 mV, which has a lower magnitude than that of *S. cerevisiae* ($\zeta_P = -30.9$), the resulting $v_{EP}^{(1)}$ of the *E. coli* cells toward the inlet (reversed direction) will be lower, allowing the smaller *E. coli* cells to migrate at a higher overall \mathbf{v}_P than the larger *S. cerevisiae* cells. These results are analogous to those in Separation 1, where the smaller polystyrene particle (2 µm) migrated faster that the larger particles (5.1 µm). The particles in Separation 1 were strategically selected to mimic the cells in Separation 2 as closely as possible. As expected from the ζ_P values of the cells, *E. coli* cells (green) migrated faster than *S. cerevisiae* as shown in the image in **Figure 2A** and the electropherogram in **Figure 2B** obtained at $\Delta V = 1000 V$ between

reservoirs B and D. The retention times were $t_{R1,e}$ = 166 s and $t_{R2,e}$ = 230 s for the *E. coli* and *S. cerevisiae* cells, respectively; and a Rs = 2.13 was obtained, indicating a complete separation. The efficiency in terms of N/meter were: N_I/m = 1,102 plates/m and N_2/m = 20,826 plates/m for *E. coli* and *S. cerevisiae*, respectively, which are comparable to those obtained with CE systems.⁵⁴ Similar to Separation 1, care was taken to ensure that the separation took place mainly under the linear EK regime, since lower voltages are preferable when handling cells. In this case, the difference between the ζ_P values, 5.5 mV, was sufficient to allow for the separation to occur mainly under the linear regime. The separation was enhanced by nonlinear EP effects. As shown in **Figure S3C-3D**, which depicts the velocities resulting from all four EK phenomena considered here, for *S. cerevisiae* cells, the nonlinear EK phenomenon of EP⁽³⁾ had a moderate effect over the overall cell velocity (\mathbf{v}_P) that aided the separation. The reproducibility of this separation in terms of $t_{R,e}$ was excellent, as only a 2% deviation for each cell type was found between repetitions (**Table S7**).

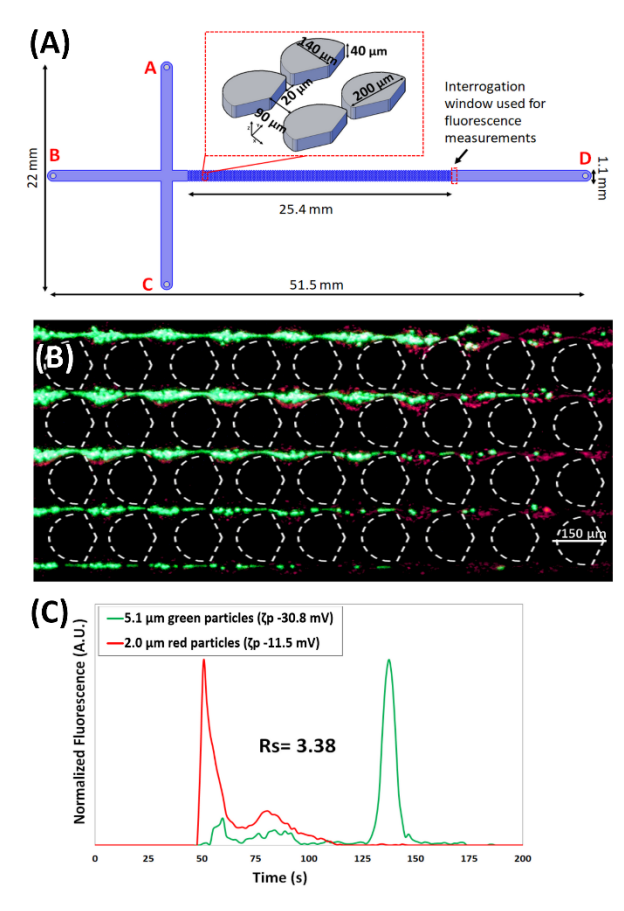


Figure 1. (A) Schematic representation of the microchannel employed in this study, depicting the dimensions of the channel and insulating posts and the location of the interrogation window used for fluorescence measurements for electropherograms, (B) Image of the microparticles as they begin to separate in "zones" within the post array at $\Delta V = 1500 V$ between reservoirs B & D. The image illustrates that the red particles migrating ahead of the green particles. (C) Electropherogram of the microparticle separation built from fluorescence signals. A video of this separation is included as supplementary information. Video S1.mp4.

The deviation between experimental results and computational modeling, shown in **Table 3**, are 20% and 27% for the *E. coli* ($t_{R1,p}$ = 132 s) and yeast cells ($t_{R2,p}$ = 169 s), respectively. These results are encouraging, since, as explained above, no correction factors were utilized to manipulate modeling results. Observations during separation experiments may explain these errors. It was observed that *E. coli* cells form aggregates when exposed to the

electric field. These aggregates behave like larger particles in the channel, which can explain some of the deviations from predicted behavior. The formation of cell aggregates was decreased by vortexing the cell sample suspension prior to injection, but it was impossible to completely eliminate aggregation. These aggregates were not observed for yeast cells. Another factor that may contribute to the deviations from COMSOL predictions in this separation is the shape of these cells, as yeast cells are almost spherical while *E. coli* cells are spheroids. Thus, besides charge and size differences between the two cell types, the shape differences could have also played a role in this separation. These results agree with literature that the separation of cells in different domains is feasible because of the substantial differences in cell envelope characteristics.³⁷

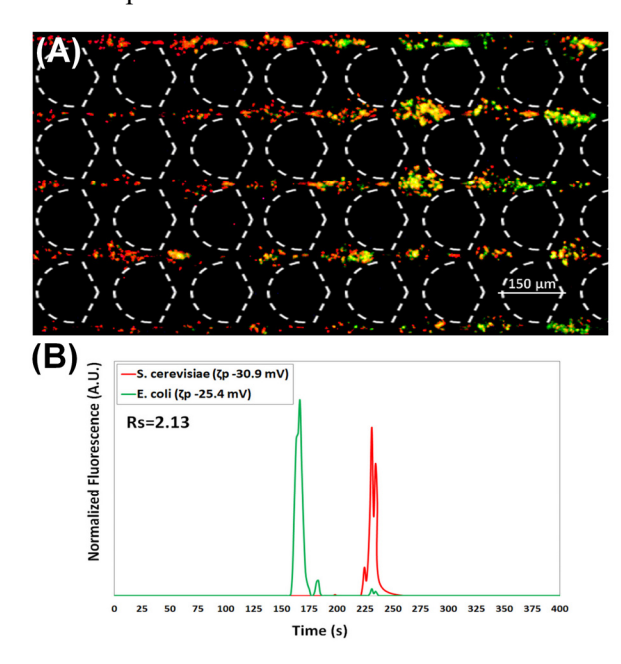


Figure 2. (A) Separation of the cells of different domains mimicked in separation 1, *E. coli* and *S. cerevisiae* cells. Image of the cells as they begin to separate in "zones" within the post array at $\Delta V = 1000 V$ between reservoirs B & D. *E. coli* cells are labelled green and *S. cerevisiae* cells are labeled red. The image illustrates the green *E. coli* cells migrating ahead of the *S. cerevisiae* cells. (B) Electropherogram between *E. coli* cells and *S. cerevisiae* cells built from fluorescence signals. A video of this separation is included as supplementary information Video_S2.mp4.

Separation of Cells of Different Domains, Prokaryotic and Eukaryotic, that are Closer in Size: *B. cereus* cells vs. *S. cerevisiae* cells. The third separation analyzed two cell types of different domains but closer in size (*B. cereus* vs. *S. cerevisiae*) than those in Separation 2. As mentioned, this project features four separations with an increasing degree of difficulty. Based on the cells' characteristics (**Table 1**) and the model predictions of retention time (**Table S5**), it was expected that *S. cerevisiae* cells would elute first, since they have a lower magnitude ζ_P value. **Figure 3A**, taken at the beginning of the post array, illustrates two regions: yeast cells (red color) are migrating ahead of *B. cereus* cells. **Figure 3B** shows the electropherogram of this separation, which confirms the expected results from ζ_P value and the cell migration in **Figure 3A**, with the red peak containing the *S. cerevisiae* cells eluting at $t_{R1,e}$ = 152 s while *B. cereus* cells eluted at $t_{R2,e}$ = 411 s at ΔV = 500 V between reservoirs B and D (**Table 3**). Separation 3 had a resolution of Rs = 3.52, indicating a complete separation between the two cell types. The efficiency in terms of N/meter were: N_1/m = 10,227 plates/m and N_2/m = 7187 plates/m which are highly competitive, and perhaps superior, to those obtained with CE systems. Separation 3 took place mainly under the linear EK regime, since as shown in the velocity predictions in **Figure S3(E-F)**, nonlinear EP (EP⁽³⁾) is mildly influencing the overall velocity, and thus, retention time of *S. cerevisiae* cells only. The standard deviation between three repetitions (**Table S7**)

was only 7% for both cells, illustrating excellent reproducibility. It is important to note that the second peak in **Figure 3B** has some "fronting", *i.e.*, some *B. cereus* cells leaked out of the post array earlier. A potential cause for this leakage is the high concentration of the cell suspension sample, which causes an additional distorting of the electric field, as the cells themselves acts as insulators, creating localized zones of higher field strength, which in turn accelerates the elution of the cells.

By comparing modeling and experimental results in terms of retention time, the COMSOL predicted times were $t_{R1,p}$ = 179 s and $t_{R2,p}$ = 357 s for the *S. cerevisiae* and *B. cereus cells* respectively, which was expected based on ζ_P values. The differences between model predicted $t_{R,p}$ and experimentally obtained $t_{R,e}$ values are below 20% for both particles, illustrating good agreement, especially considering that the model does not account for injection bias or cell-cell interactions. Other groups have reported continuous cell separations, Kang *et al.*⁵⁹ worked on the size-selective separation of white blood cells and breast cancer cells, which had a difference in volume of ~9,000 μ m³. In Separation 3, the difference in the spheroids' volume is only 110 μ m³, a much smaller difference than that exploited by Kang *et al.*⁵⁹. In a similar report, Cetin *et al.*,⁶⁰ separated yeast cells (3-5 μ m diameter) and white blood cells (8-12 μ m diameter) in an electrode-based microfluidic device. As reported in **Table 1**, the cells used in Separation 3 are closer in size, with yeast cells having a diameter of 6.23 μ m, and *B. cereus* being a 4.86 x 1.94 μ m rod. These results illustrate that carefully designed iEK systems can discriminate and effectively separate cell of similar characteristics.

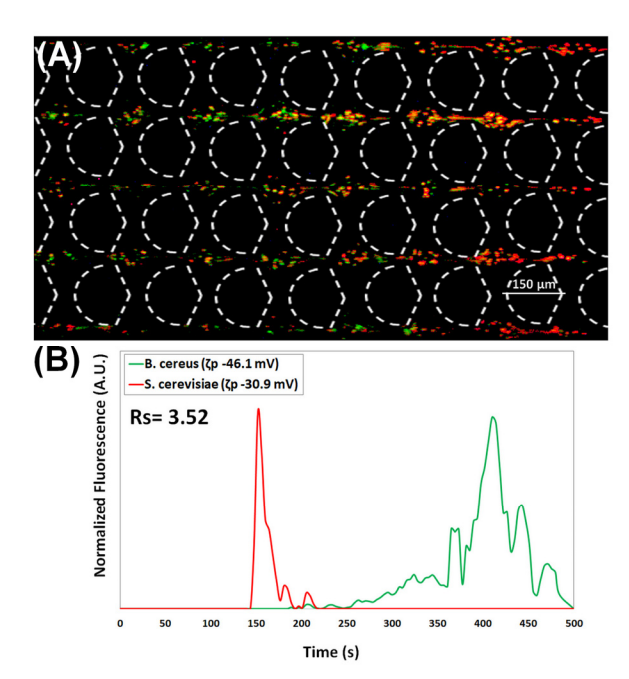


Figure 3. (A) Separation of cells of different domains: prokaryotic bacteria and eukaryotic, *B. cereus* bacterial cells vs. *S. cerevisiae* cells. Image of the cells within the post array at $\Delta V = 500 V$ between reservoirs B & D. *S. cerevisiae* cells are labelled red and *B. cereus* cells are labelled green. (B) Electropherogram between *B. cereus* and *S. cerevisiae* cells built from fluorescence signals. A video of this separation is included as supplementary information Video S3.mp4.

Separation of Cells of the Same Genus: *B. cereus* vs. *B. subtilis* Cells. The final separation was focused on separating cells of the same genus, *B. subtilis* and *B. cereus* cells. From the ζ_P values reported in **Table 1**, this separation can take place by exploiting the difference in ζ_P values. The difference of 16.1 mV would allow *B. subtilis* cells to elute first since their ζ_P has a lower magnitude. After selecting the appropriate voltages employing COMSOL simulations, Separation 4 was carried out as illustrated in **Figure 4(A-B)** at an applied $\Delta V = 500 V$

between reservoirs B and D (Table 3). The image in Figure 4A shows the cells in the middle of the post array where B. subtilis cells (red, shown in yellow due to photobleaching) and B. cereus cells (green) are starting to separate, with B. subtilis cells migrating ahead. Figure 4B shows the electropherogram of Separation 4, where the two peaks are observed, with retention times of $t_{R1,e}$ = 170 s and $t_{R2,e}$ = 460 s for B. subtilis and B. cereus, respectively. This large difference in retention time enabled a high separation resolution of Rs = 4.79, and a high separation efficiency in terms of N/meter of $N_1/m = 23,220$ plates/m and $N_2/m = 15,411$ plates/m which is highly competitive when compared to those obtained with CE systems. 54 These results are highly encouraging, as this the most challenging separation in this study. Separation 4 was influenced by nonlinear EP, since the overall velocity, and thus the retention time, of B. subtilis cells was moderately affected by EP⁽³⁾, as depicted in the velocity plots in Figure S3(G-H). This is expected, as B. subtilis has a very high value of $\mu_{EP,NL}^{(3)}$, therefore it was critical to keep this separation mainly under linear EK regime. By selecting an overall electric field of 97.1 V/cm (resulting from $\Delta V = 500 \, V$, Table S6), the effects of EP⁽³⁾ were kept moderate, ensuring that B. subtilis could elute first; increasing the applied voltage could decrease the difference between retention times, destroy the separation, an even reverse the elution order. As shown in **Table S6**, under an applied $\Delta V = 600 V B$. subtilis cells start to trap within the post array, which is highly undesirable as the separation is continuous, taking place under the streaming EK regime. Excellent reproducibility was obtained, with variations between repetitions in terms of retention time $(t_{R,e})$ of only 6% and 13% (**Table 3**) for *B. subtilis* and *B. cereus* cells, respectively.

Regarding the agreement between modeling and experimental results (**Table 3**), the predicted values are $t_{R1,p}$ = 180 s for *B. subtilis* and $t_{R2,p}$ = 357 s for *B. cereus* cells. These findings are in agreement with experimental results, as the deviations are -6% and 22% only, for *B. subtilis* and *B. cereus* cells, respectively. The development of cell aggregates, which were observed during the experiments, can certainly contribute to these deviations, as the aggregates can partially clog the channel, affecting the overall migration of the cells. Aggregates were more significant during the elution of *B. cereus* cells, which have the higher deviation (22%). Moreover, as discussed above, these modeling results were obtained without any manipulation to the model by adding correction factors. The model developed here is a useful tool for designing and selecting the appropriate conditions for carrying out cell separations. The model in this work has great flexibility, it can be used under linear and nonlinear regimes since it fully accounts for the effects of linear and nonlinear EK phenomena.

Other groups have reported the separation of similar cells. In 2008, Beck *et al.*⁶¹ employed planar electrodes and DEP effects to discriminate between spores of bacillus species. They analyzed *B. cereus*, *Bacillus mycoides* (*B. mycoides*), *Bacillus licheniformis* (*B. licheniformis*), and *B. subtilis* spores employing impedance analysis to measure electrical current changes, proving effective discrimination at the single cell level. However, this study did not include the elution of the separated fractions. Employing a g-iDEP system, Jones *et al.*²³ isolated three serotypes of *E. coli* bacteria (O6:K1:H1, O55:H7, and O157:H7), the cells were successfully identified within the channel, but were not eluted as separated fractions. More recently, Liu and Hayes⁶² worked on the separation of two serotypes of *Salmonella* named sv. *Cubana* and sv. *Poona* also utilizing a g-iDEP device. They demonstrated the complete differentiation of intact sv. *Poona* and sv. *Cubana* cells. Nonetheless, each strain was monitored individually in the microfluidic device and no elution of the separated fractions was reported. Our group³⁷ has demonstrated the trapping of *B. cereus* and *B. subtilis* employing iEK with insulating posts of different shapes (circle-shaped posts), but this is the first report of effective cell separation in a continuous streaming EK regime, where separated fractions were successfully eluted from the post array. The present work is the first report on effective continuous iEK-based separations of three distinct binary mixtures of cells, where the quality of the separations was assessed in terms of $t_{R,e}$, Rs and *N/meter* values. Furthermore, this is also the first report of three

distinct cells separations with Rs > 1.5, that includes good agreement between model predicted and experimentally obtained cell retention times in an iEK system.

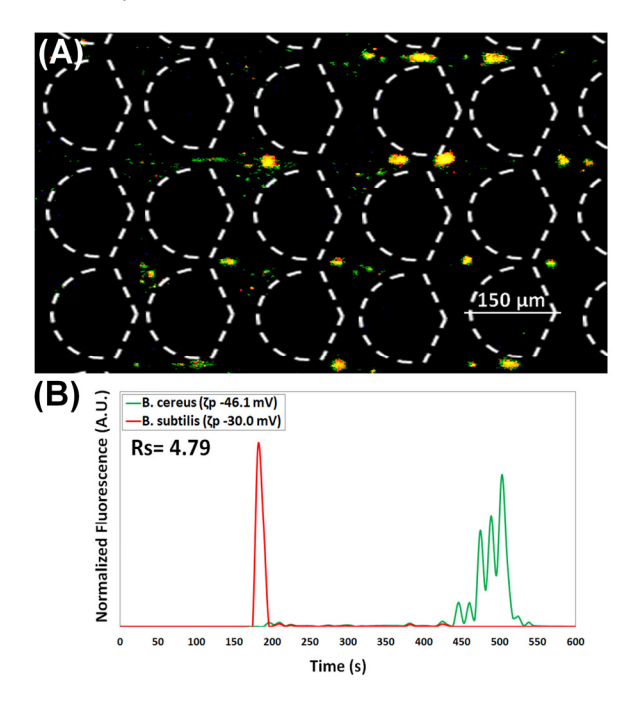


Figure 4. (A) Image of the separated cells after they have created two distinguished "zones" within the post array at $\Delta V = 500 V$ between reservoirs B & D. B. subtilis cells are labeled red (but appear yellow due to photobleaching) and B. cereus cells are labelled green. The image depicts B. subtilis cells migrating ahead than B. cereus cells, illustrating the separation process. (B) Electropherogram between cells of the same genus, B. cereus and B. subtilis, built from fluorescence signal. A video of this separation is included as supplementary information Video S4.mp4.

CONCLUSIONS

384

385

386

387

388

389

390

391

392

393

394

395

396

397

398

399

400

401

402

403

404

405

406

407

408

This research studied the separation of microparticles and cells employing a combination of linear and nonlinear EK effects in an iEK microfluidic system. A total of four distinct separations were carried out with increasing level of difficulty. First, the separation of E. coli and yeast cells was mimicked by separating microparticles of different sizes (2 µm and 5.1 µm). Then, the separation of E. coli and yeast was accomplished by leveraging the knowledge from the microparticle separation. Two more separations were performed, a separation of cells in different domains: B. cereus vs. S. cerevisiae; and a separation between cells of the same genus B. cereus vs. B. subtilis. Modeling was employed to select the appropriate conditions for each one of the four separations reported here, and the modeling results, in term of retention time, were in good agreement with experimental results. The quality of the separations was assessed by employing the parameters of Rs and separation efficiency in terms of N/meter; in all four cases Rs > 1.5, illustrating well-resolved separations, and the separation efficiencies in N/meter were competitive to those obtained with CE systems. This is the first report on effective continuous iEK separations of three distinct binary mixtures of cells, combining linear and nonlinear EK phenomena within the same device, which enables a highly discriminatory separation schemes.. The present study included mathematical modeling and experimental demonstrations, where modeling results, in terms of retention time, were in good agreement with experimental results. Furthermore, by considering particles/cells characteristics (assessed a priori), model predictions allowed identifying the appropriate EK regime (linear or nonlinear) and required potential for

- 409 each separation. This work demonstrates that iEK systems have the capacity to effectively discriminate and separate
- cells of very similar characteristics in matter of minutes; including separations of cells of the same genus where the
- separated fractions were successfully eluted from the post array.

ASSOCIATED CONTENT

Supporting information

- The supplementary file contains Tables S1-S7 and Figures S1-S3. Additionally, the video files Video S1.mp4,
- Video S2.mp4, Video S3.mp4, and Video S4.mp4 are also included. These videos depict simultaneously the
- elution of the particles/cells and the acquisition of the fluorescence as a function of time.

AUTHOR INFORMATION

- 418 Corresponding Author
- Blanca H. Lapizco-Encinas Microscale Bioseparations Laboratory and Biomedical Engineering Department,
- Rochester Institute of Technology, Rochester, New York14623, United States; orcid.org/0000-0001-6283-8210;
- 421 Email: <u>bhlbme@rit.edu</u>
- 422 Authors

412

413

417

- 423 Alaleh Vaghef-Koodehi-Microscale Bioseparations Laboratory and Biomedical Engineering Department,
- Rochester Institute of Technology, Rochester, New York14623, United States
- Olivia D. Ernst -Microscale Bioseparations Laboratory and Biomedical Engineering Department, Rochester
- Institute of Technology, Rochester, New York 14623, United States
- 427 Author Contributions
- 428 AVK: Experimentation, Data Analysis, Writing Original Draft Review & Editing. ODE: Experimentation, Data
- 429 Analysis, Writing Original Draft Review & Editing. BHLE: Conceptualization, Methodology, Project
- administration, Supervision, Writing Original Draft Review & Editing.
- 431 Notes

433

438

The authors declare no competing financial interest.

ACKNOWLEDGMENTS

- This material is based upon work supported by the National Science Foundation under award CBET-2127592.
- The authors would like to acknowledge Curran Dillis for his initial experimental support with this project. The
- 436 authors would like to acknowledge Braulio Cardenas-Benitez for insightful and helpful discussions about nonlinear
- electrophoresis.

REFERENCES

439 (1) Rajapaksha, P.; Elbourne, A.; Gangadoo, S.; Brown, R.; Cozzolino, D.; Chapman, J. A Review of Methods for the

- Detection of Pathogenic Microorganisms. *Analyst*. Royal Society of Chemistry January 21, 2019, pp 396–411. https://doi.org/10.1039/c8an01488d.
- 442 (2) Horká, M.; Karásek, P.; Růžička, F.; Dvořáčková, M.; Sittová, M.; Roth, M. Separation of Methicillin-Resistant from
 443 Methicillin-Susceptible Staphylococcus Aureus by Electrophoretic Methods in Fused Silica Capillaries Etched with
 444 Supercritical Water. *Anal. Chem.* **2014**, *86* (19), 9701–9708. https://doi.org/10.1021/ac502254f.
- (3) Horká, M.; Šalplachta, J.; Karásek, P.; Růžička, F.; Štveráková, D.; Pantůček, R.; Roth, M. Rapid Isolation, Propagation, and Online Analysis of a Small Number of Therapeutic Staphylococcal Bacteriophages from a Complex Matrix. ACS
 Infect. Dis. 2020, 6 (10), 2745–2755. https://doi.org/10.1021/acsinfecdis.0c00358.
- (4) Horká, M.; Štveráková, D.; Šalplachta, J.; Šlais, K.; Šiborová, M.; Růžička, F.; Pantůček, R. Electrophoretic Techniques
 for Purification, Separation and Detection of Kayvirus with Subsequent Control by Matrix-Assisted Laser
 Desorption/Ionization Time-of-Flight Mass Spectrometry and Microbiological Methods. *J. Chromatogr. A* 2018, 1570,
 155–163. https://doi.org/10.1016/j.chroma.2018.07.078.

453

454

455

456

457

458

459

460

461

462

463

464

468

469

470

471

472

473

474

475

476

477

478

479

480

481

482 483

484

485

486

490

491

492

- (5) Dziubakiewicz, E.; Buszewski, B. Applications of Electromigration Techniques: Electromigration Techniques in Detection of Microorganisms. In *Electromigration Techniques: Theory and Practice*; Buszewski, B., Dziubakiewicz, E., Szumski, M., Eds.; Springer Berlin Heidelberg: Berlin, Heidelberg, 2013; pp 287–298. https://doi.org/10.1007/978-3-642-35043-6 16.
- (6) Buszewski, B.; Maślak, E.; Złoch, M.; Railean-Plugaru, V.; Kłodzińska, E.; Pomastowski, P. A New Approach to Identifying Pathogens, with Particular Regard to Viruses, Based on Capillary Electrophoresis and Other Analytical Techniques. TrAC - Trends Anal. Chem. 2021, 139. https://doi.org/10.1016/J.TRAC.2021.116250.
- (7) Rogowska, A.; Pomastowski, P.; Złoch, M.; Railean-Plugaru, V.; Król, A.; Rafińska, K.; Szultka-Młyńska, M.; Buszewski, B. The Influence of Different PH on the Electrophoretic Behaviour of Saccharomyces Cerevisiae Modified by Calcium Ions. *Sci. Rep.* **2018**, *8* (1), 7261. https://doi.org/10.1038/s41598-018-25024-4.
- (8) Buszewski, B.; Król, A.; Pomastowski, P.; Railean-Plugaru, V.; Szultka-Młyńska, M. Electrophoretic Determination of Lactococcus Lactis Modified by Zinc Ions. *Chromatographia* 2019, 82 (1), 347–355. https://doi.org/10.1007/s10337-018-3665-3.
- 465 (9) W. Armstrong, D.; Schulte, G.; M. Schneiderheinze, J.; J. Westenberg, D. Separating Microbes in the Manner of
 466 Molecules. 1. Capillary Electrokinetic Approaches. *Anal. Chem.* **1999**, 71 (24), 5465–5469.
 467 https://doi.org/10.1021/ac990779z.
 - (10) Lapizco-Encinas, B. H. Microscale Nonlinear Electrokinetics for the Analysis of Cellular Materials in Clinical Applications: A Review. *Microchim. Acta* **2021**, *188* (3), 104. https://doi.org/10.1007/s00604-021-04748-7.
 - (11) Vaghef-Koodehi, A.; Lapizco-Encinas, B. H. Microscale Electrokinetic-Based Analysis of Intact Cells and Viruses. *Electrophoresis* **2022**, *43* (1–2), 263–287. https://doi.org/10.1002/elps.202100254.
 - (12) Guo, W.; Tao, Y.; Liu, W.; Song, C.; Zhou, J.; Jiang, H.; Ren, Y. A Visual Portable Microfluidic Experimental Device with Multiple Electric Field Regulation Functions. *Lab Chip* **2022**, *22* (8), 1556–1564. https://doi.org/10.1039/D2LC00152G.
 - (13) Liu, W.; Tao, Y.; Xue, R.; Song, C.; Wu, Q.; Ren, Y. Continuous-Flow Nanoparticle Trapping Driven by Hybrid Electrokinetics in Microfluidics. *Electrophoresis* **2021**, *42* (7–8), 939–949. https://doi.org/10.1002/ELPS.202000110.
 - (14) Perez-Gonzalez, V. H. Particle Trapping in Electrically Driven Insulator-Based Microfluidics: Dielectrophoresis and Induced-Charge Electrokinetics. *Electrophoresis* **2021**, *42* (23), 2445–2464. https://doi.org/10.1002/elps.202100123.
 - (15) Lapizco-Encinas, B. H. The Latest Advances on Nonlinear Insulator-Based Electrokinetic Microsystems under Direct Current and Low-Frequency Alternating Current Fields: A Review. *Analytical and Bioanalytical Chemistry*. Springer October 19, 2022, pp 885–905. https://doi.org/10.1007/s00216-021-03687-9.
 - (16) Luo, J.; Muratore, K. A.; Arriaga, E. A.; Ros, A. Deterministic Absolute Negative Mobility for Micro- and Submicrometer Particles Induced in a Microfluidic Device. *Anal. Chem.* **2016**, *88* (11), 5920–5927. https://doi.org/10.1021/acs.analchem.6b00837.
 - (17) Khair, A. S. Nonlinear Electrophoresis of Colloidal Particles. *Current Opinion in Colloid and Interface Science*. Elsevier March 25, 2022, p 101587, https://doi.org/10.1016/j.cocis.2022.101587.
- 487 (18) Cardenas-Benitez, B.; Jind, B.; Gallo-Villanueva, R. C.; Martinez-Chapa, S. O.; Lapizco-Encinas, B. H.; Perez-Gonzalez,
 488 V. H. Direct Current Electrokinetic Particle Trapping in Insulator-Based Microfluidics: Theory and Experiments. *Anal. Chem.* **2020**, *92* (19), 12871–12879. https://doi.org/10.1021/acs.analchem.0c01303.
 - (19) Oh, M.; Jayasooriya, V.; Woo, S. O.; Nawarathna, D.; Choi, Y. Selective Manipulation of Biomolecules with Insulator-Based Dielectrophoretic Tweezers. *ACS Appl. Nano Mater.* **2020**, *3* (1), 797–805. https://doi.org/10.1021/acsanm.9b02302.
- 493 (20) Jones, P. V.; Salmon, G. L.; Ros, A. Continuous Separation of DNA Molecules by Size Using Insulator-Based 494 Dielectrophoresis. *Anal. Chem.* **2017**, *89* (3), 1531–1539. https://doi.org/10.1021/acs.analchem.6b03369.
 - (21) Gallo-Villanueva, R. C.; Rodríguez-López, C. E.; Díaz-de-la-Garza, R. I.; Reyes-Betanzo, C.; Lapizco-Encinas, B. H.

- DNA Manipulation by Means of Insulator-Based Dielectrophoresis Employing Direct Current Electric Fields. Electrophoresis **2009**, 30 (24), 4195–4205. https://doi.org/10.1002/elps.200900355.
- 498 (22) Shi, L.; Kuhnell, D.; Borra, V. J.; Langevin, S. M.; Nakamura, T.; Esfandiari, L. Rapid and Label-Free Isolation of Small
 499 Extracellular Vesicles from Biofluids Utilizing a Novel Insulator Based Dielectrophoretic Device. *Lab Chip* **2019**, *19*500 (21), 3726–3734. https://doi.org/10.1039/c9lc00902g.
- 501 (23) Jones, P. V.; DeMichele, A. F.; Kemp, L. K.; Hayes, M. A. Differentiation of *Escherichia Coli* Serotypes Using DC Gradient Insulator Dielectrophoresis. *Anal. Bioanal. Chem.* **2014**, *406* (1), 183–192. https://doi.org/10.1007/s00216-013-7437-5.

505

506

507

508

509

513

514

515

516

517

518

519

520

521

522

523524

525

526

527

528

529

530

531

532

533

534

535

536

537

538

544545

- (24) Saucedo-Espinosa, M. A.; Lalonde, A.; Gencoglu, A.; Romero-Creel, M. F.; Dolas, J. R.; Lapizco-Encinas, B. H. Dielectrophoretic Manipulation of Particle Mixtures Employing Asymmetric Insulating Posts. *Electrophoresis* **2016**, *37* (2), 282–290. https://doi.org/10.1002/elps.201500195.
- (25) Liu, Y.; Jiang, A.; Kim, E.; Ro, C.; Adams, T.; Flanagan, L. A.; Taylor, T. J.; Hayes, M. A. Identification of Neural Stem and Progenitor Cell Subpopulations Using DC Insulator-Based Dielectrophoresis. *Analyst* **2019**, *144* (13), 4066–4072. https://doi.org/10.1039/c9an00456d.
- 510 (26) Zhang, X.; Xu, X.; Ren, Y.; Yan, Y.; Wu, A. Numerical Simulation of Circulating Tumor Cell Separation in a
 511 Dielectrophoresis Based Y-Y Shaped Microfluidic Device. Sep. Purif. Technol. 2021, 255, 117343.
 512 https://doi.org/10.1016/J.SEPPUR.2020.117343.
 - (27) Ding, J.; Lawrence, R. M.; Jones, P. V.; Hogue, B. G.; Hayes, M. A. Concentration of Sindbis Virus with Optimized Gradient Insulator-Based Dielectrophoresis. *Analyst* **2016**, *141* (6), 1997–2008. https://doi.org/10.1039/C5AN02430G.
 - (28) Hilton, S. H.; Crowther, C. V.; McLaren, A.; Smithers, J. P.; Hayes, M. A. Biophysical Differentiation of Susceptibility and Chemical Differences in Staphylococcus Aureus. *Analyst* **2020**, *145* (8), 2904–2914. https://doi.org/10.1039/C9AN01449G.
 - (29) Crowther, C. V.; Hilton, S. H.; Kemp, L. K.; Hayes, M. A. Isolation and Identification of *Listeria Monocytogenes* Utilizing DC Insulator-Based Dielectrophoresis. *Anal. Chim. Acta* **2019**, *1068*, 41–51. https://doi.org/10.1016/j.aca.2019.03.019.
 - (30) Jones, P. V.; Huey, S.; Davis, P.; Yanashima, R.; McLemore, R.; McLaren, A.; Hayes, M. A. Biophysical Separation of *Staphylococcus Epidermidis* Strains Based on Antibiotic Resistance. *Analyst* **2015**, *140* (15), 5152–5161. https://doi.org/10.1039/c5an00906e.
 - (31) Zellner, P.; Shake, T.; Hosseini, Y.; Nakidde, D.; Riquelme, M. V.; Sahari, A.; Pruden, A.; Behkam, B.; Agah, M. 3D Insulator-Based Dielectrophoresis Using DC-Biased, AC Electric Fields for Selective Bacterial Trapping. *Electrophoresis* **2015**, *36* (2), 277–283. https://doi.org/10.1002/elps.201400236.
 - (32) Nakidde, D.; Zellner, P.; Alemi, M. M.; Shake, T.; Hosseini, Y.; Riquelme, M. V.; Pruden, A.; Agah, M. Three Dimensional Passivated-Electrode Insulator-Based Dielectrophoresis. *Biomicrofluidics* **2015**, *9* (1), 14125. https://doi.org/10.1063/1.4913497.
 - (33) Braff, W. A.; Willner, D.; Hugenholtz, P.; Rabaey, K.; Buie, C. R. Dielectrophoresis-Based Discrimination of Bacteria at the Strain Level Based on Their Surface Properties. *PLoS One* **2013**, *8* (10), e76751. https://doi.org/10.1371/journal.pone.0076751.
 - (34) Hill, N.; Lapizco-Encinas, B. H. Continuous Flow Separation of Particles with Insulator-Based Dielectrophoresis Chromatography. *Anal. Bioanal. Chem.* **2020**, *412* (16), 3891–3902. https://doi.org/10.1007/s00216-019-02308-w.
 - (35) Miller, A.; Hill, N.; Hakim, K.; Lapizco-encinas, B. H. Fine-tuning Electrokinetic Injections Considering Nonlinear Electrokinetic Effects in Insulator-based Devices. *Micromachines* **2021**, *12* (6), 628. https://doi.org/10.3390/mi12060628.
- 539 (36) Hill, N.; De Peña, A. C.; Miller, A.; Lapizco-Encinas, B. H. On the Potential of Microscale Electrokinetic Cascade 540 Devices. *Electrophoresis* **2021**, *42* (23), 2474–2482. https://doi.org/10.1002/elps.202100069.
- (37) Coll De Peña, A.; Miller, A.; Lentz, C. J.; Hill, N.; Parthasarathy, A.; Hudson, A. O.; Lapizco-Encinas, B. H. Creation of
 an Electrokinetic Characterization Library for the Detection and Identification of Biological Cells. *Anal. Bioanal. Chem.* 2020, 412 (16), 3935–3945. https://doi.org/10.1007/s00216-020-02621-9.
 - (38) Vaghef-Koodehi, A.; Dillis, C.; Lapizco-Encinas, B. H. High-Resolution Charge-Based Electrokinetic Separation of Almost Identical Microparticles. *Anal. Chem.* **2022**, *94* (17), 6451–6456. https://doi.org/10.1021/ACS.ANALCHEM.2C00355.
- 547 (39) Moncada-Hernández, H.; Lapizco-Encinas, B. H. Simultaneous Concentration and Separation of Microorganisms: 548 Insulator-Based Dielectrophoretic Approach. *Anal. Bioanal. Chem.* **2010**, 396 (5), 1805–1816. 549 https://doi.org/10.1007/s00216-009-3422-4.
- 550 (40) Antunez-Vela, S.; Perez-Gonzalez, V. H.; Coll De Peña, A.; Lentz, C. J.; Lapizco-Encinas, B. H. Simultaneous 551 Determination of Linear and Nonlinear Electrophoretic Mobilities of Cells and Microparticles. *Anal. Chem.* **2020**, *92*

- (22), 14885–14891. https://doi.org/10.1021/acs.analchem.0c03525.
- (41) Coll De Peña, A.; Hill, N.; Lapizco-Encinas, B. H. Determination of the Empirical Electrokinetic Equilibrium Condition of Microorganisms in Microfluidic Devices. *Biosensors* **2020**, *10* (10), 148. https://doi.org/10.3390/bios10100148.
- 555 (42) Kang, Y.; Cetin, B.; Wu, Z.; Li, D. Continuous Particle Separation with Localized AC-Dielectrophoresis Using Embedded 556 Electrodes and an Insulating Hurdle. *Electrochim. Acta* **2009**, *54* (6), 1715–1720. 557 https://doi.org/10.1016/j.electacta.2008.09.062.
 - (43) Kale, A.; Malekanfard, A.; Xuan, X. Curvature-Induced Dielectrophoretic Particle Manipulation Systems. *Micromachines* **2020**, *11* (7), 707. https://doi.org/10.3390/mi11070707.
 - (44) DuBose, J.; Lu, X.; Patel, S.; Qian, S.; Joo, S. W.; Xuan, X. Microfluidic Electrical Sorting of Particles Based on Shape in a Spiral Microchannel. *Biomicrofluidics* **2014**, *8* (1), 1–8. https://doi.org/10.1063/1.4862355.
 - (45) Kale, A.; Malekanfard, A.; Xuan, X. Analytical Guidelines for Designing Curvature-Induced Dielectrophoretic Particle Manipulation Systems. *Micromachines* **2020**, *11* (7), 707. https://doi.org/10.3390/mi11070707.
 - (46) Weirauch, L.; Giesler, J.; Baune, M.; Pesch, G. R.; Thöming, J. Shape-Selective Remobilization of Microparticles in a Mesh-Based DEP Filter at High Throughput. *Sep. Purif. Technol.* **2022**, *300*, 121792. https://doi.org/10.1016/J.SEPPUR.2022.121792.
 - (47) Pesch, G. R.; Du, F.; Schwientek, U.; Gehrmeyer, C.; Maurer, A.; Thöming, J.; Baune, M. Recovery of Submicron Particles Using High-Throughput Dielectrophoretically Switchable Filtration. *Sep. Purif. Technol.* **2014**, *132*, 728–735. https://doi.org/https://doi.org/10.1016/j.seppur.2014.06.028.
 - (48) Calero, V.; García-Sánchez, P.; Ramos, A.; Morgan, H. Electrokinetic Biased Deterministic Lateral Displacement: Scaling Analysis and Simulations. *J. Chromatogr. A* **2020**, *1623*, 461151. https://doi.org/10.1016/j.chroma.2020.461151.
 - (49) Calero, V.; Garcia-Sanchez, P.; Honrado, C.; Ramos, A.; Morgan, H. AC Electrokinetic Biased Deterministic Lateral Displacement for Tunable Particle Separation. *Lab Chip* **2019**, *19* (8), 1386–1396. https://doi.org/10.1039/c8lc01416g.
 - (50) Tottori, S.; Misiunas, K.; Keyser, U. F.; Bonthuis, D. J. Nonlinear Electrophoresis of Highly Charged Nonpolarizable Particles. *Phys. Rev. Lett.* **2019**, *123* (1), 14502. https://doi.org/10.1103/PhysRevLett.123.014502.
 - (51) Rouhi Youssefi, M.; Diez, F. J. Ultrafast Electrokinetics. *Electrophoresis* **2016**, *37* (5–6), 692–698. https://doi.org/10.1002/elps.201500392.
 - (52) Saucedo-Espinosa, M. A.; Lapizco-Encinas, B. H. Refinement of Current Monitoring Methodology for Electroosmotic Flow Assessment under Low Ionic Strength Conditions. *Biomicrofluidics* **2016**, *10* (3), 033104. https://doi.org/10.1063/1.4953183.
 - (53) Lalonde, A.; Romero-Creel, M. F.; Lapizco-Encinas, B. H. Assessment of Cell Viability after Manipulation with Insulator-Based Dielectrophoresis. *Electrophoresis* **2015**, *36* (13), 1479–1484. https://doi.org/10.1002/elps.201400331.
 - (54) Beckman, J.; Song, Y.; Gu, Y.; Voronov, S.; Chennamsetty, N.; Krystek, S.; Mussa, N.; Li, Z. J. Purity Determination by Capillary Electrophoresis Sodium Hexadecyl Sulfate (CE-SHS): A Novel Application For Therapeutic Protein Characterization. *Anal. Chem.* **2018**, *90* (4), 2542–2547. https://doi.org/10.1021/acs.analchem.7b03831.
 - (55) Breadmore, M. C. Electrokinetic and Hydrodynamic Injection: Making the Right Choice for Capillary Electrophoresis. *Bioanalysis*. Future Science Ltd 2009, pp 889–894. https://doi.org/10.4155/bio.09.73.
 - (56) Saucedo-Espinosa, M. A.; Lapizco-Encinas, B. H. Exploiting Particle Mutual Interactions To Enable Challenging Dielectrophoretic Processes. *Anal. Chem.* **2017**, *89* (16), 8459–8467. https://doi.org/10.1021/acs.analchem.7b02008.
 - (57) Hill, N.; Lapizco-Encinas, B. H. On the Use of Correction Factors for the Mathematical Modeling of Insulator Based Dielectrophoretic Devices. *Electrophoresis* **2019**, *40* (18–19), 2541–2552. https://doi.org/10.1002/elps.201900177.
 - (58) Gong, M.; Wehmeyer, K. R.; Stalcup, A. M.; Limbach, P. A.; Heineman, W. R. Study of Injection Bias in a Simple Hydrodynamic Injection in Microchip CE. *Electrophoresis* **2007**, 28 (10), 1564–1571. https://doi.org/10.1002/elps.200600616.
- 596 (59) Kang, Y.; Li, D.; Kalams, S. A.; Eid, J. E. DC-Dielectrophoretic Separation of Biological Cells by Size. *Biomed. Microdevices* **2008**, *10* (2), 243–249. https://doi.org/10.1007/s10544-007-9130-y.
 - (60) Çetin, B.; Kang, Y.; Wu, Z.; Li, D. Continuous Particle Separation by Size via AC-Dielectrophoresis Using a Lab-on-a-Chip Device with 3-D Electrodes. *Electrophoresis* **2009**, *30* (5), 766–772. https://doi.org/10.1002/elps.200800464.
 - (61) Beck, J. D.; Shang, L.; Li, B.; Marcus, M. S.; Hamers, R. J. Discrimination between Bacillus Species by Dielectrophoretically Positioned Spores. *Spore* **2008**, *80* (10), 3757–3761. https://doi.org/10.1021/ac702113t.
- 602 (62) Liu, Y.; Hayes, M. A. Differential Biophysical Behaviors of Closely Related Strains of Salmonella. *Front. Microbiol.* 2020, *11*, 302. https://doi.org/10.3389/FMICB.2020.00302.

Table of Contents Only

